PAPER

# A cladding-pumping based power-scaled noise-like and dissipative soliton pulse fiber laser

To cite this article: Zhiguo Lv *et al* 2023 *Chinese Phys. B* **32** 024207

# A cladding-pumping based power-scaled noise-like and dissipative soliton pulse fiber laser

Zhiguo Lv(吕志国)[1], Hao Teng(滕浩)[2,3,†], and Zhiyi Wei(魏志义)[2,3,4,‡]

[1] *School of Physical Science and Technology, Inner Mongolia Key Laboratory of Nanoscience and Nanotechnology, Inner Mongolia University, Hohhot* 010021, *China*

[2] *Beijing National Laboratory for Condensed Matter Physics, Institute of Physics, Chinese Academy of Sciences, Beijing* 100190, *China*

[3] *Songshan Lake Materials Laboratory, Dongguan* 523808, *China*

[4] *University of Chinese Academy of Sciences, Beijing* 100049, *China*

(Received 21 April 2022; revised manuscript received 5 August 2022; accepted manuscript online 5 September 2022)

We report a high-average-power noise-like pulse (NLP) and dissipative soliton (DS) pulse fiber laser. Average power as high as 4.8 W could be obtained at the fundamental mode-locked repetition rate. The NLP can also be transformed into a more powerful DS mode-locking state by optimizing the polarization and losses of intra-cavity pulses in the nonlinear polarization evolution regime. The operation mode between the NLP and DS can be switched, and the laser output performance in both modes has been studied. The main advantage of this work is switchable high-power operation between the NLP and DS. In comparison with conventional single-mode NLP fiber lasers, the multi-function high-power optical source will greatly push its application in supercontinuum generation, coherence tomography, and industrial processing.

**Keywords:** cladding pumping, high power, noise-like pulse, dissipative soliton

**PACS:** 42.55.–f, 42.55.Wd, 42.65.Re, 42.60.Fc **DOI:** 10.1088/1674-1056/ac8f3e

## 1. Introduction

With the development of ultrashort pulse lasers continually moving in the minimization, portable and flexible direction, mode-locked fiber lasers have attracted considerable attention and have been thoroughly researched in the past. In addition to nonlinear systems that are used to generate coherent pulses[1] for fundamental science and application fields, passively mode-locked fiber lasers can be treated as ideal platforms to research and explore various unstable phenomena and soliton dynamics.[2–4] Typically, under the guidance of the complex Ginzburg–Landau equation, various intriguing nonlinear processes, such as soliton rain,[5] soliton molecules,[6] soliton resonance,[7] soliton explosion,[8] and rogue wave[9] have been extensively experimentally investigated in conventional single-mode fiber lasers.

In scientific research, power-scaled and energy-enhanced mode-locked fiber lasers are very favorable for suppression of amplified spontaneous emission (ASE), and simultaneously beneficial for improvement of the signal to noise ratio (SNR) in reduced-repetition-rate energetic laser systems. However, there are some difficulties associated with directly obtaining such laser performance. In mode-locked fiber lasers, the obtainable maximum average power and pulse energy are relevant to dispersion and nonlinear phase accumulation. As a result, fiber-based mode-locking pulses have been forced from the conventional soliton in the anomalous dispersion domain to the dissipative soliton (DS) in the all-normal-dispersion domain, bypassing stretched-pulse and similariton regimes. Therefore, all-normal-dispersion mode-locking is one of the most promising schemes to support more powerful and energetic ultrashort pulse generation due to a chirped-pulse spectral filtering-based DS shaping mechanism.[10] Beyond this, there is also another type of operational behavior in mode-locked fiber lasers that can extend the average power/pulse energy, namely, noise-like pulse (NLP) generation. Due to the potential to possess higher average power and larger pulse energy, NLP operation in the all-normal-dispersion domain has been a significant research subject in recent years.[11]

Since they were first demonstrated,[12] different wavelength NLP fiber lasers (1030 nm, 1550 nm, 2000 nm) have been intensively studied.[13–16] Due to their unique forms and inherent laser characteristics, such as quasi stable packets, double-scale temporal behavior, and low temporal coherence, most of the research works on NLP generation mainly focus on the realization methods,[17,18] generation mechanisms,[19–21] and nonlinear dynamics.[22,23] In contrast, the related research works on high-power NLP generation are relatively rarely reported. However, in some potential applications, such as supercontinuum generation,[24] material processing,[25] and optical coherence tomography,[26] power-scaled and energy-increment NLP mode-locked seed sources are greatly desired. Therefore, research on high-power NLP fiber lasers has important practical significance. It is well known that in conventional core-pumped single-mode lasers, the NLP is limited in

†Corresponding author. E-mail: hteng@iphy.ac.cn

‡Corresponding author. E-mail: zywei@iphy.ac.cn

 http://iopscience.iop.org/cpb http://cpb.iphy.ac.cn

average power and pulse energy due to low pump power.[27] In addition, intense nonlinear phase-accumulation-induced pulse splitting is a key restriction factor for power scaling and energy enhancement.[28] For example, pump power less than 1 W will induce pulse splitting for a cavity length as short as 9 m.[29] As a result, for most of the reported single-mode NLP mode-locked fiber lasers, the output power is less than 1 W in normal dispersion mode at 1 μm with an NPE-based fiber cavity. Based on an Yb-doped 10/125 double-clad gain fiber, average power up to 1.4 W has been realized in a nonlinear optical loop mirror mode-locked oscillator.[30] Therefore, reasonably increasing the mode-field diameter is an effective method for scaling the average power and pulse energy, and alleviating nonlinearity.[31,32] Moreover, combiner fused spliced cladding pumping employing high-power multimode laser diodes has also been proved to be a viable method to significantly enhance the pump capacity and laser gain factor.[33]

Therefore, in consideration of its inherent performance advantages and potential application prospects, we conduct research on the generation of a high-average-power mode-locked NLP in a large-core-diameter flexible fiber-based laser configuration, in which a cladding pumping scheme with a high-power multimode laser diode has been utilized to significantly promote the power increase. With such enhanced performance construction, the average power up to 4.8 W at $\sim 63.28$ MHz repetition rate has been experimentally obtained. Meanwhile, the recorded power fluctuations are better than 3% RMS over 8 hours. Further, by optimizing the polarization and losses of intra-cavity pulses in the nonlinear polarization evolution regime, the power-scaled NLP operation state can also be switched to stable DS mode-locking. The detailed laser performance has also been studied.

## 2. Experiment setup

The cladding-pumping-based dual-mode fiber laser is schematically shown in Fig. 1. In the configuration, the polarization beam splitter (PBS) acts as the main output port for the power-scaled NLP and DS lasers, and the ejection port from the polarization-dependent optical isolator (PD-ISO) acts as the mode-locked monitoring port. The gain medium is a 1.2 m long Yb-doped double-clad fiber (YBDCF) with 10 μm core diameter and 125 μm cladding diameter. The nominal peak cladding absorption is 7.4 dB/m @976 nm and the maximum launched pump power from the available multimode laser diode is 29 W. The rest of the components in the ring cavity all have 10 μm core diameter and 125 μm cladding diameter (Nufern: LMA-GSF-10/125-M) and the total passive fiber length in the experiment is 1.8 m. Enough laser gain can be obtained by cladding coupling the multimode pump into the YBDCF through a $(2+1)\times 1$ pump combiner. The PD-ISO ensures intra-cavity pulse unidirectional operation along the ring oscillator in the clockwise direction, which is formed by a pair of reverse-placed fiber collimators. The polarization-dependent spectral filter is formed by sandwiching the birefringent plate (BFP) between the PD-ISO and the PBS. The experimentally utilized BFP is 3 mm thickness, and thus the estimated filtering bandwidth is about 20 nm. To obtain stable NLP mode-locking operation, the quarter-wave plate (QWP) and half-wave plate (HWP) need to be respectively properly adjusted. With such structure improvement, including the enhancement of pump capacity and reasonable control of nonlinearity, the laser performance on the NLP, especially average power, has been elevated to the utmost extent in terms of the current parameter settings. Furthermore, due to the fact that the transmittance of the NPE varies with the orientation of the wave plates, when most of the instantaneous power of the intra-cavity laser reaches the saturation threshold of the cavity-parameter-related NPE, the NLP operation state can also be easily switched to conventional DS mode-locking. In contrast with the previous reported research on NLPs, in addition to the direct high-average-power output, the switchable operation mode between the NLP and DS is the main advantage of this work.

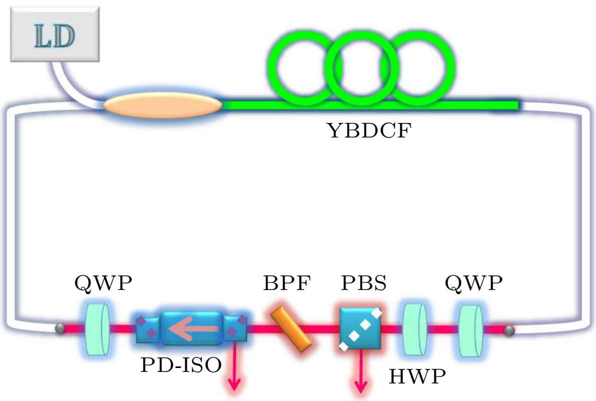


**Fig. 1.** A schematic of the proposed dual-mode mode-locked fiber laser. QWP: quarter-wave plate; HWP: half-wave plate; PBS: polarizing beam splitter; BFP: birefringent plate; PD-ISO: polarization-dependent isolator; YBDCF: Yb-doped double-clad gain fiber; LD: laser diode.

## 3. Results and discussion

With the presented experimental configuration, both power-scaled NLP and DS pulses can be achieved. These two kinds of different operation modes are carefully studied in terms of power tendency, spectral characteristics, temporal distribution and power stability over 8 h. Initially, the stable and self-started mode-locked NLP is obtained under a pump power of 5.9 W. During the process, besides manipulation of the polarization of intra-cavity pulses, the coupling efficiency between these two reverse-placed fiber collimators needs to be optimized to regulate the intra-cavity losses and match the NLP generation conditions. Figure 2(a) shows the stable mode-locked pulse train, which is characterized using a fast photodetector (EOT3000, 2 GHz bandwidth) coupled to a 600 MHz oscilloscope (RIGOL MSO8064). The pulse train features equal-amplitude and uniformly-spaced temporal distribution, and demonstrates the mode-locked stability.

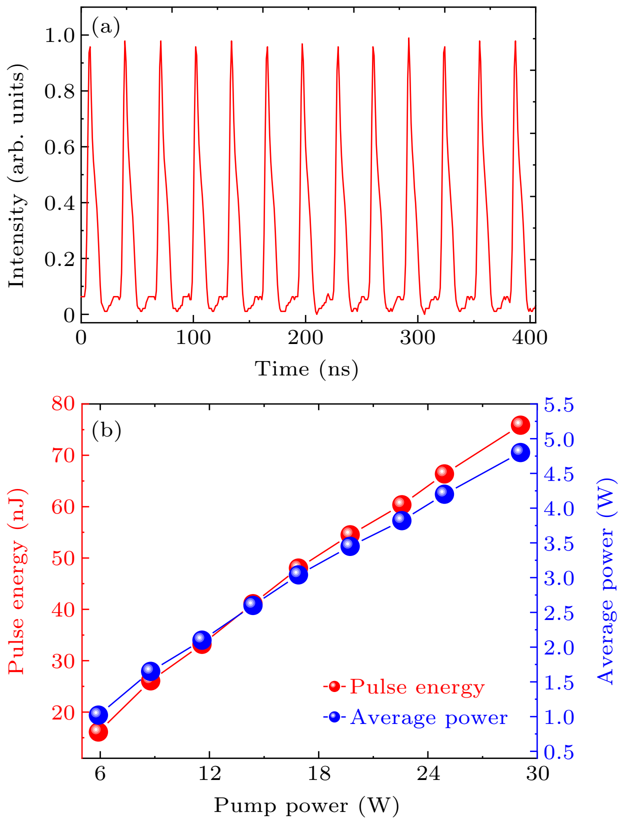


**Fig. 2.** (a) The mode-locked NLP pulse train; (b) pump power dependence of NLP output power and pulse energy at 63.28 MHz fundamental repetition rate.

In the studied pump-power range, the experimentally obtainable maximum output powers at the main port from the PBS and ejection port from the PD-ISO are 4.8 W and 432 mW, respectively. For NLP mode-locking, to initiate pulsed operation, the intra-cavity saturable losses are larger due to its wider pulse widths and weaker peak power. Figure 2(b) indicates the NLP increased output power and pulse energy at the main port at $\sim$ 63.28 MHz repetition rate. With the increment in pump power, the energy of the NLP continuously increases from 16 nJ (1.02 W) to 75.8 nJ (4.8 W) and without pulse splitting. The spectra are centered at 1072.7 nm and the resulting 3 dB spectral bandwidths are 29.6 nm. Figure 3(a) shows the measured spectra with 0.2 nm resolution on linear and logarithmic (inset) scales, respectively. The spectral characteristics are measured using an optical spectrum analyzer (Yokogawa AQ6370C). The spectra profiles are prominently distinguished from that of the conventional DS with steep-edge spectral distribution. The reason for this can be attributed to the inadequate pulse-shaping of the intra-cavity laser and reverse saturable absorption of the NLP. Adopting an intensity autocorrelator (APE PulseCheck), we measure the autocorrelation traces of the NLP under the maximum output power of 4.8 W. The measured results are shown in Fig. 3(b). From the results, we obtain the central coherent spike with a pulse duration as short as 115 fs, which is located on the top of a wide pedestal with 23 ps full width at half-maximum. The femtosecond spike in the picosecond wave packets originates from the lack of phase coherence across the pulse train with randomly varying amplitude and phase fluctuations.

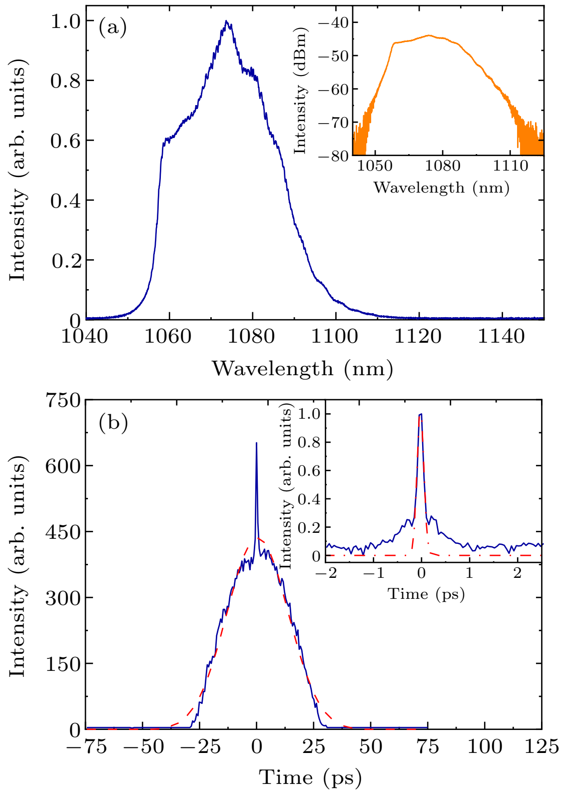


**Fig. 3.** (a) Mode-locked NLP output spectra respectively shown on linear and logarithmic (inset) scales; (b) measured NLP autocorrelation traces in the scanning range of 150 ps. The inset shows the autocorrelation trace of the central spike. The red dashed lines in (b) correspond to Gauss fitting.

Further, we also measure the NLP power stability with regard to its importance in practical use. For instance, in most fiber laser applications, power stability is one of the extremely important performance metrics and determines the application range of fiber lasers to a large extent. Therefore, to more accurately reflect the operation performance of the cladding-pumping-based NLP fiber laser operating in the all-normal-dispersion domain, the stability over 8 hours was measured and is shown in Fig. 4(a). The calculated root-mean-square (RMS) fluctuations are 0.9% under 4.8 W output power. Although the used gain fiber supports three modes, we obtain strictly fundamental transverse mode distribution in the experiment due to the fact that the fundamental mode has larger peak power density and more intense nonlinear saturable absorption compared with higher-order modes.

After obtaining stable NLP mode-locking, for further optimization of waveplate orientations under a pump power of 8.77 W, the NLP operation mode then can be switched to DS mode-locking. In contrast to the NLP, the generation of DS pulses is attributed to enough modulation in the temporal and spectral domain as a result of NPE and the dissipative filtering mechanism. Figure 5 presents the power and pulse energy variations with increasing pump power. In the experimentally studied pump range from 8.77 W to 29 W, a stable single DS pulse can be constantly maintained, which is in accordance with the NLP case. Under a pump power of 29 W, the obtainable maximum power and pulse energy are 4.86 W and 76.7 nJ at the main port, respectively.

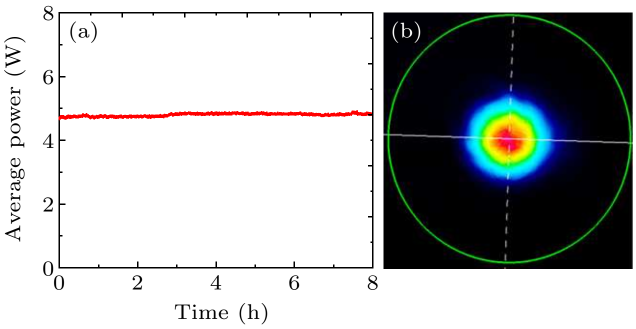


**Fig. 4.** Power stability and beam profile measurement of the NLP under 4.8 W output power.

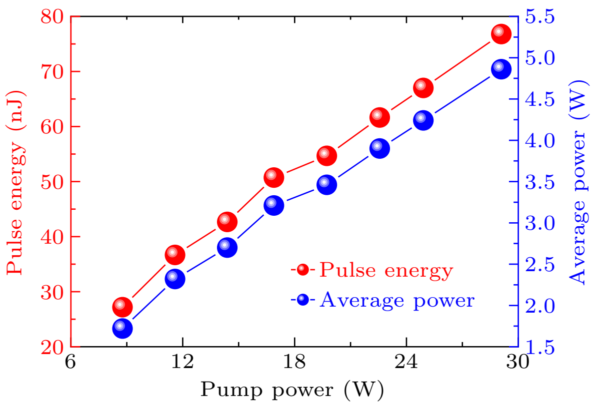


**Fig. 5.** Increased DS power and pulse energy as functions of pump power at $\sim$ 63.28 MHz fundamental repetition rates.

The spectra are centered at 1074.9 nm and the 3 dB spectral bandwidths are 28 nm. The chirped pulse widths are measured using an APE intensity autocorrelator and are shown in Fig. 6(a). The pulse widths are 6.9 ps assuming Gauss fitting. Pulse duration as short as 141 fs can be obtained as chirped pulses pass through a 1000 lines/mm transmission grating-pair compressor. The autocorrelation traces corresponding to compressed pulses are shown in Fig. 6(b). The inset in Fig. 6(b) corresponds to mode-locked DS spectra with a sharp steep-edge as a result of dissipative spectral filtering.

In contrast to the NLP, in the DS mode-locked operation, in addition to the 4.86 W power output at the main port, average power up to 3.2 W can be obtained from the ejection port of the PD-ISO. For NLP mode-locking, the saturable losses are larger than those of DS mode-locking due to wider pulse widths and weaker peak power. In contrast, for DS mode-locking due to enough modulation in the temporal and spectral domain, the non-saturable losses are more than those of NLP mode-locking. As a result, we obtain a total of 8.06 W mode-locked output power at both the main port and the ejection port of the PD-ISO. Likewise, for the high-average-power mode-locked DS laser, we measure the power stability over 8 h at the main port. The measured RMS fluctuations are 0.9%, demonstrating the excellent operational performance.

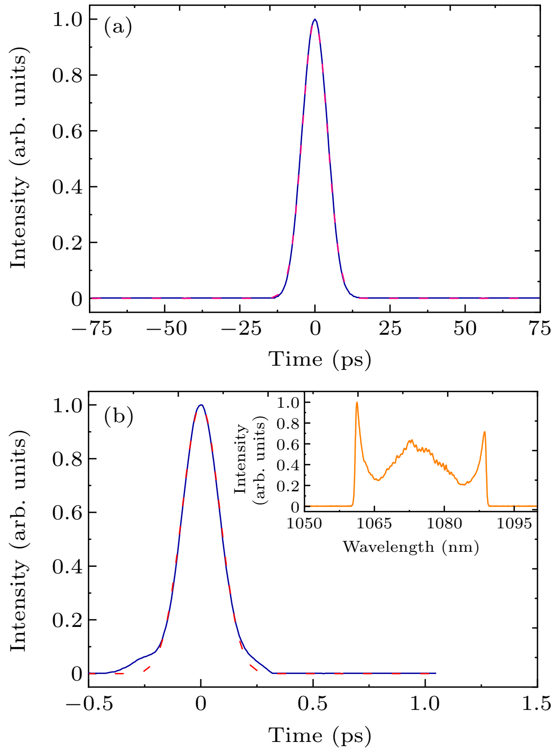


**Fig. 6.** (a) Measured chirped autocorrelation traces at the main port and shown by the blue solid line; (b) measured autocorrelation traces for compressed pulses and shown by the blue solid line; the red dashed lines correspond to Gauss fitting.

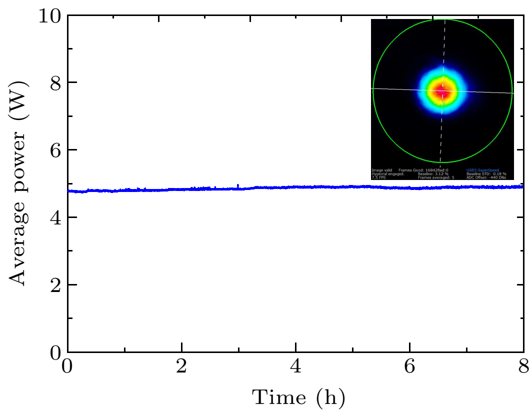


**Fig. 7.** Power stability measurement for DS pulses from the main port over 8 h. The inset shows the beam profile of the compressed DS pulses.

## 4. Conclusion

In summary, we experimentally demonstrate an effective and viable method to generate a high average-power NLP laser directly from a mode-locked fiber oscillator. By choosing a filter with suitable spectral bandwidth, and reasonable optimization of polarization and losses of intra-cavity pulses, average power up to 4.8 W is obtained based on a cladding-pumping scheme with a high-power multimode laser diode. Moreover, NLP operation mode can also be switched to DS mode-locking with a comparable power level. Benefiting from low nonlinearity and a powerful pump, the output power from the presented laser configuration is much greater than that of conventional single-mode fiber lasers. The high-power dual-mode (NLP and DS) optical source will greatly push its application in supercontinuum generation, coherence tomography, and industrial processing.

## Acknowledgments

Project supported by the National Natural Science Foundation of China (Grant No. 12164030), the Major Program of the National Natural Science Foundation of China (Grant No. 12034020), Young Science and Technology Talents of Inner Mongolia, China (Grant No. NJYT22101), and the Talent Development Fund of Inner Mongolia, China.

## References

[1] Liang C B, Song Y R, Dong Z K, Wu Y F, Tian J R and Xu R Q 2020 *Chin. Phys. B* **29** 074206
[2] Liu X M, Yao X K and Cui Y D 2018 *Phys. Rev. Lett.* **121** 023905
[3] Zhao J Q, Zhou J, Li L, Klimczak M, Komarov A, Su L, Tang D Y, Shen D Y and Zhao L M 2019 *Opt. Express* **27** 29770
[4] Gao J J, Ning T Y, Liu Y J, Shang X X, Han X L, Guo Q X, Guo L G, Lu Z Y, Wang Z H, Zhang H J and Jiang S Z 2019 *Appl. Opt.* **58** 7897
[5] Sulimany K, Lib O, Masri G, Klein A, Fridman M, Grelu P, Gat O, Steinberg H 2018 *Phys. Rev. Lett.* **121** 133902
[6] Stratmann M, Pagel T and Mitshke F 2005 *Phys. Rev. Lett.* **95** 143902
[7] Li D J, Li L, Zhou J Y, Zhao L M, Tang D Y and Shen D Y 2016 *Sci. Rep.* **6** 23631
[8] Gurevich S V, Schelte C and Javaloyes J 2019 *Phys. Rev. A* **99** 061803
[9] Klein A, Masri G, Duadi H, Sulimany K, Lib O, Steinberg H, Kolpakov S A and Fridman M 2018 *Optica* **5** 774
[10] Andy C, Willian H R and Frank W W 2008 *J. Opt. Soc. Am. B* **25** 140
[11] Wang X F, Xia Q and Gu B 2019 *Opt. Commun.* **434** 180
[12] Horowitz M, Barad Y and Silberberg Y 1997 *Opt. Lett.* **22** 799
[13] Li D J, Shen D Y, Li L, Chen H, Tang D Y and Zhao L M 2015 *Opt. Express* **23** 25889
[14] Li X L, Zhang S M, Han M M and Liu J M 2017 *Opt. Lett.* **42** 4203
[15] Li J F, Zhang Z X, Sun Z Y, Luo H Y, Liu Y, Yan Z J, Mou C B, Zhang L and Turitsyn S K 2014 *Opt. Express* **22** 7875
[16] Wu T Y, Dou Z Y, Zhang B and Hou J 2020 *Chin. Phys. B* **29** 014202
[17] Li J F, Yan Z J, Sun Z Y, Luo H Y, He Y L, Li Z, Liu Y and Zhang L 2014 *Opt. Express* **22** 31020
[18] Chen Y, Wu M, Tang P H, Chen S Q, Du J, Jiang G B, Li Y, Zhao C J, Zhang H and Wen S C 2014 *Laser Phys. Lett.* **11** 055101
[19] Tang D Y, Zhao L M and Zhao B 2005 *Opt. Express* **13** 2289
[20] Zhao L M, Tang D Y, Wu J, Fu X Q and Wen S C 2007 *Opt. Express* **15** 2145
[21] Kobtsev S, Kukarin S, Smirnov S, Turitsyn S and Latkin A 2009 *Opt. Express* **17** 20707
[22] Hernandez H S, Pottiez O, Sanchez M D, Tamayo R I A, Cruz J P L, Hernandez J C, Escamilla B I and Kuzin E A 2015 *Opt. Express* **23** 18840
[23] Sanchez E G, Pottiez O, Rodriguez Y B, Cruz J P L, Villalon H E I, Garcia J C H, Jimenez M B and Kuzin E A 2016 *Opt. Express* **24** 18917
[24] Luo X, Tuan T H, Saini T S, Nguyen H P T, Suzuki T and Ohishi Y 2019 *IEEE Photo. Tech. Lett.* **31** 1225
[25] Ozgören K, Öktem B, Yilmaz S, IIday F Ö and Eken K 2011 *Opt. Express* **19** 1764
[26] Huang D, Swanson E A, Lin C P, Schuman J S, Stinson W G, Chang W, Hee M R, Flotte T, Gregory K, Puliafito C A and Fujimoto J G 1991 *Science* **254** 1178
[27] Wang X, Komarov A, Klimczak M, Su L, Tang D Y, Shen D Y, Li L and Zhao L M 2019 *Opt. Express* **27** 24147
[28] Boucon A, Barvlau B, Fatome J, Finot C, Sylvestre T, Lee M W, Grelu P and Millot G 2012 *Appl. Phys. B* **106** 283
[29] Lv Z G, Teng H, Wang L N, Wang R and Wei Z Y 2015 *Chin. Phys. Lett.* **32** 084201
[30] Chen H, Chen S P, Jiang Z F and Hou J 2015 *Opt. Lett.* **40** 5490
[31] Lv Z G, Teng H, Wang L N, Wang R, Wang J L and Wei Z Y 2015 *Chin. Phys. B* **24** 114203
[32] Lv Z G, Teng H, Wang L N, Wang J L and Wei Z Y 2016 *Chin. Phys. B* **25** 094208
[33] Lv Z G, Yang Z, Yang X J, Li F, Li Q L, Wang Y S, Zhao W and Wei Y F 2018 *Laser Phys. Lett.* **15** 115109